Effect of Natural Convection on Spontaneous Combustion of Coal Stockpiles

Spontaneous combustion may occur in a coal stockpile when the heat generated within the pile cannot be dissipated at near ambient temperature. Under practical conditions, natural convection enhances the rate of heat removal from the bed and shifts the ignition to lower particle sizes (higher reactivities). Analysis of three limiting cases of a one-dimensional model yields criteria predicting the conditions under which ignition occurs as well as those for which a low-temperature (extinguished) state exists for all particle sizes. A simple asymptotic relation predicts the ignition point at large Rayleigh numbers.

Kevin Brooks, Vemuri Balakotaiah, Dan Luss
Department of Chemical Engineering
University of Houston
Houston, TX 77004

Introduction

Spontaneous combustion of stockpiled coal—a highly undesirable event—has been studied extensively in the last century. The coal is heated due to oxidation and moisture adsorption (Schmal et al., 1985) and spontaneous combustion occurs when the heat released within the pile cannot be dissipated at near ambient temperatures. Most previous studies were concerned mainly with the intrinsic heat generation, which can be measured by several techniques, such as the crossing point method or calorimetry (Schmidt and Elder, 1940).

Sondreal and Ellman (1974), Nordon (1979), and Schmal et al. (1985) developed models accounting for the coupled transport and reaction rates in coal stockpiles. All these models assume that a prescribed flow exists in the bed, and are rather similar to the axial dispersion model of a packed-bed reactor, for which multiplicity is known to exist (Hlavacek and Votruba, 1977; Varma and Aris, 1977). As expected, these models predict that coal piles may reach different steady states under certain conditions.

Natural convection plays a key role in the self-ignition of reactive materials. Merzhanov and Shtessel (1973) examined in a classic paper the effect of natural convection on the thermal explosion of liquid mixtures in square domains. Kordylewski and Krajewski (1984) analyzed self-ignition in a closed cylindrical geometry. Recently, Viljoen and Hlavacek (1987) examined reaction-induced convection in a closed rectangular box. These studies have shown that the possibility of thermal explosion decreases with increasing Rayleigh number and that explosion may be prevented by vigorous natural convection. A comprehensive review of experimental and theoretical studies of oxidative self-heating (spontaneous combustion) of several materials was presented by Bowes (1984).

Previous studies of self-ignition of reactive materials were mostly in closed systems and assumed a constant permeability and that the reaction (heat generation) rate was independent of the particle size. Young et al. (1986) have examined natural convection in coal stockpiles with variable reaction rate. Brooks and Glasser (1986) presented recently a one-dimensional model which assumed that natural convection was the primary flow mechanism, that is, the flow was induced by buoyancy and not by an imposed external pressure gradient. Thus, a different flow rate corresponds to each steady state solution. This behavior is another illustration of *thermoflow multiplicity*, many examples of which were described by Lee et al., (1987). That model predicts that under certain conditions either a low-temperature (extinguished) or a high-temperature (ignited) state can be obtained, while for others only an ignited or an extinguished state exists.

The goal of this study is to determine the multiplicity features of a one-dimensional model in order to obtain simple criteria predicting the conditions under which the desired extinguished state exists for all particle sizes and when a transition to the ignited state (combustion) occurs at some particle size. This information is valuable for determining the key parameters, which affect the spontaneous ignition and the sensitivity of the ignition to the values of these parameters. The information gained by the study of the one-dimensional model is expected to be a useful guide in the analysis of more realistic and intricate models of spontaneous combustion.

The current address of Kevin Brooks is Department of Chemical Engineering, University of Witwatersrand, Wits, 2050 South Africa.

Development of a Mathematical Model

A coal pile usually has a conical or flat-topped shape. Thus, a three-dimensional model is needed to describe its behavior. To simplify the analysis and to obtain simple criteria predicting the key factors that affect self-ignition, we consider a coal pile having the shape of a slab, the length and width of which are much larger than its height. Thus, we use a one-dimensional model that accounts only for vertical variation in the state variables.

We describe the slab by a pseudohomogeneous model ignoring mass dispersion. That is, we assume that $u \gg D_e/L$, where u is the velocity through the bed and D_e is the effective diffusivity of oxygen. Strictly speaking, the molar flow rate in the bed is not constant, as the oxygen is adsorbed at low temperatures without producing gaseous products (Itay, 1984). Moreover, the variation of pressure and temperature in the bed causes a change in density and hence in velocity. This change in the molar flow is usually rather small and it is ignored in the species and energy balances.

The oxygen, energy, and momentum balances are:

$$\frac{u_o \rho_a}{M} \frac{dy}{dx} = -r \tag{1}$$

$$k_e \frac{d^2T}{dx^2} - u_o \rho_a c_p \frac{dT}{dx} + (-\Delta H) r = 0 \tag{2}$$

$$\frac{dP^*}{dx} = -f_p + \rho_a g \left(1 - \frac{T_a}{T}\right) - \frac{\rho_a u_o^2}{T_a} \frac{dT}{dx} \tag{3}$$

where P^* is the small difference between the pressure in the bed and ambient pressure, and u_o is the velocity at the bottom of the layer ($x = 0$). Its value is selected so that it can satisfy the Eqs. 1–3 and the corresponding boundary conditions. The last term in Eq. 3 accounts for the pressure change due to gas expansion. This term is usually very small relative to the others and was neglected in this work.

The intrinsic reaction rate is assumed to be linear with respect to the oxygen partial pressure, and to be proportional to a, the reactive surface area per unit volume of bed, i.e.,

$$r = k_o \exp(-E/RT) a \frac{P_a y}{RT} \tag{4a}$$

We assume here that the pile consists of nonporous coal particles and that the reaction occurs only on the external surface of the pellets so that

$$r = \frac{6k_o}{D_p}(1 - \epsilon) \exp(-E/RT) \frac{P_a y}{RT_a} \triangleq k(T)(1 - \epsilon)\left(\frac{y}{D_p}\right) \tag{4b}$$

The analysis can readily be modified to handle the more general case in which the reaction rate is defined by Eq. 4a and to account for any impact of intraparticle diffusional limitations. The frictional pressure drop is calculated using only the first term in the Ergun equation, neglecting the second because the Reynolds number is usually very small. Assuming that the viscosity is independent of temperature,

$$f_p = \frac{150\mu}{D_p^2} \frac{(1 - \epsilon)^2}{\epsilon^3} u = \frac{\mu}{\kappa} u \tag{5}$$

where the permeability κ is defined by

$$\kappa = \frac{\epsilon^3 D_p^2}{150(1 - \epsilon)^2} \tag{6}$$

The boundary conditions at $x = 0$ (bottom of coal layer) are

$$k_e \frac{dT}{dx} = (u_o \rho_a c_p + h_o)(T - T_a) \tag{7a}$$

$$y = y_a \tag{7b}$$

$$P^* = 0 \tag{7c}$$

while at $x = L$ (top of the coal layer)

$$k_e \frac{dT}{dx} = -h_1(T - T_a) \tag{8a}$$

$$P^* = 0 \tag{8b}$$

We assume that heat is lost from the coal bed by natural convection as well as by radiation and forced convection from its surface. Thus, the conditions of Eqs. 7a and 8a include heat loss terms that are not normally included in the axial dispersion model. For simplicity we assume $h_0 = h_1$ in this work.

As in other thermoflow problems, the velocity in this model is not specified. Thus, in order to determine it one has to specify two boundary conditions for the momentum balance, which is a first-order differential equation. There exist at most several values of the velocity that satisfy Eqs. 1–3 and the associated boundary conditions, Eqs. 7 and 8.

This model is somewhat similar to the pseudohomogeneous axial-dispersion model of a packed-bed reactor. One major difference is that in this model the flow is not prescribed and is due to buoyancy rather than an imposed external pressure gradient. Moreover, the momentum and energy balances are coupled in this case, and as shown by Lee et al. (1987), this may lead to multiplicity even when no axial feedback of heat by conduction exists in the packed bed.

We shall examine here two questions that are of practical interest:

1. Under what conditions does an extinguished state exist for all particle sizes?
2. If this is not the case, what is the particle size at which ignition occurs?

To carry out the analysis we introduce the following dimensionless parameters:

$$Y = \frac{y}{y_a} \qquad \theta = \frac{T}{T_a}$$

$$\Pi = \frac{P^*}{\rho_a g L} \qquad X = \frac{x}{L}$$

$$U_r = \frac{k_e}{\rho_a c_p L} \qquad S = \frac{u_o}{U_r}$$

$$\gamma = \frac{E}{RT_a} \qquad \beta = \frac{(-\Delta H) y_a}{M c_p T_a}$$

$$\phi_h^2 = \frac{k(T_a)(1-\epsilon)L^2Mc_p}{k_eD_p} = \frac{t_\lambda}{t_g} \qquad Bi = \frac{Lh}{k_e} = \frac{t_\lambda}{t_r}$$

$$Ra = \frac{\rho_a^2 g c_p L D_p^2 \epsilon^3}{150\mu k_e(1-\epsilon)^2} = \frac{\kappa g \rho_a}{\mu U_r} = \frac{t_\lambda}{t_c} \qquad t_\lambda = \frac{L^2\rho_a c_p}{k_e}$$

$$t_g = \frac{\rho_a D_p}{k(T_a)(1-\epsilon)M} \qquad t_c = \frac{\mu L}{\rho_a g \kappa}$$

$$t_r = \frac{\rho_a c_p L}{h} \tag{9}$$

The dimensionless activation energy γ is a measure of the sensitivity of the reaction (heat generation) rate to changes in the temperature. The parameter β is the dimensionless adiabatic temperature rise. Each of the dimensionless numbers that characterize the system—the thermal Thiele modulus ϕ_h^2, the Rayleigh number Ra, and the Biot number Bi—is the ratio of two characteristic times. Four characteristic times are important in this problem, those for heat conduction, t_λ, heat generation, t_g, natural convection t_c, and heat loss from the surface t_r. Simplified limiting models may be used to describe the behavior of the system when one or two of the characteristic times are much smaller than the others.

Using the above dimensionless groups, Eqs. 1–3 are transformed to

$$S\frac{dY}{dX} = -\phi_h^2 Y \exp(\gamma - \gamma/\theta) \tag{10}$$

$$\frac{d^2\theta}{dx^2} - S\frac{d\theta}{dX} + \beta\phi_h^2 Y \exp(\gamma - \gamma/\theta) = 0 \tag{11}$$

$$\frac{d\Pi}{dX} = \frac{-S\theta}{Ra} + \left(1 - \frac{1}{\theta}\right) \tag{12}$$

and the boundary conditions become

$$\frac{d\theta}{dX} = (S + Bi)(\theta - 1); \quad X = 0 \tag{13a}$$

$$Y = 1; \quad X = 0 \tag{13b}$$

$$\Pi = 0; \quad X = 0 \tag{13c}$$

$$\frac{d\theta}{dX} = -Bi(\theta - 1); \quad X = 1 \tag{14a}$$

$$\Pi = 0; \quad X = 1 \tag{14b}$$

The model Eqs. 10–14 cannot be solved analytically. It is rather difficult to gain insight into the structure of the solutions of a nonlinear model containing many parameters. Thus, we consider first three limiting simplified models, that contain fewer parameters. These simplified models are useful for gaining insight into the structure of the solutions and reducing the computational effort. We then analyze the behavior of the general model.

Analysis of Limiting Models

Lumped thermal model

When the characteristic time for heat conduction in the bed, t_λ, is much smaller than that for natural convection t_c and heat loss t_r, the temperature in the bed is essentially uniform, and the energy balance becomes an algebraic equation:

$$(S + 2Bi)(\theta - 1) = \beta S[1 - Y(1)] \tag{15a}$$

This limiting case is referred to as the "lumped thermal model." The assumption that the characteristic time for conduction is much smaller than the other two time constants is not satisfied in practice. We consider this limiting case mainly because it is the simplest nontrivial model that enables an easy analytical prediction of some important qualitative features of the general case. This limiting model predicts that the velocity and temperature are constant in the bed, and that the friction and buoyancy forces balance each other at every point. The corresponding dimensionless oxygen concentration and excess pressure balances can be brought to the form

$$Y(X) = \exp\left\{-\frac{\phi_h^2}{S}\exp\left[\gamma\left(1 - \frac{1}{\theta}\right)\right]X\right\} \tag{15b}$$

$$\Pi(X) = 0 \tag{15c}$$

The dimensionless velocity satisfies the relation

$$S = Ra\frac{(\theta - 1)}{\theta^2} \tag{15d}$$

Substituting Eqs. 15b and 15d into Eq. 15a, we find that the bed temperature must satisfy the algebraic equation

$$F(\theta, Da_r, Ra_r, \gamma, \beta) \equiv \theta - 1 + \frac{2\theta^2}{Ra_r} - \beta + \beta\exp\left[-\frac{Da_r\theta^2}{Ra_r(\theta - 1)}\exp(\gamma - \gamma/\theta)\right] = 0 \tag{16}$$

where

$$Da_r = \frac{\phi_h^2}{Bi} = \frac{t_r}{t_g} = \frac{k(T_a)(1-\epsilon)Mc_pL}{hD_p} \tag{17a}$$

$$Ra_r = \frac{Ra}{Bi} = \frac{t_r}{t_c} = \frac{\rho_a^2 g c_p \kappa}{\mu h} \tag{17b}$$

Since the velocity and concentration profiles are a unique function of the temperature, the steady state features of the lumped thermal model are determined by Eq. 16.

To examine the multiplicity features of Eq. 16 we rewrite it as

$$Da_r = \frac{Ra_r(\theta - 1)\ln\left(\dfrac{\beta}{1 + \beta - \theta - 2\theta^2/Ra_r}\right)}{\theta^2\exp(\gamma - \gamma/\theta)} \equiv G(\theta) \tag{18}$$

$G(\theta)$ is positive for all θ in $(1, \theta_m)$ where θ_m is the highest temperature that can be attained by the bed and is given by

$$\theta_m = 0.25 Ra_r[\sqrt{1 + 8(1+\beta)/Ra_r} - 1] \qquad (19a)$$

For $Ra_r \to \infty$, θ_m attains a maximum value of $1 + \beta$. The minimal value of θ_m is unity and is attained when

$$Ra_r = \frac{2}{\beta} \equiv Ra_m \qquad (19b)$$

Note that for small values of the Rayleigh number, Ra_r, (smaller or of the order of magnitude of Ra_m) the above model is not valid, as the oxygen diffusion term has to be included in the mass balance Eq. 10.

Since $G(1) = 0$ and $G(\theta_m) = \infty$, Eq. 18 must have at least one solution and the total number of solutions for any set of parameters is odd. The boundary between a unique and multiple (three) solutions for some Da_r in the (γ, β) space is the locus of the hysteresis points of Eq. 18, defined by

$$G - Da_r \frac{dG}{d\theta} = \frac{d^2G}{d\theta^2} = 0 \qquad (20)$$

Elimination of θ and Da_r from Eq. 20 gives the uniqueness boundary for all Da_r, shown in Figure 1 for several values of the parameter Ra_r. The curve for $Ra_r = \infty$ describes the "adiabatic" case ($h = 0$) in which the heat is lost from the bed only by natural convection. In this case, the uniqueness boundary approaches asymptotically $\gamma = 2$ for $\beta \gg 1$ and $\gamma\beta \approx 4.2$ for $\beta \ll 1$. The uniqueness boundary for any finite Ra_r lies above that for $Ra_r = \infty$ and to the right of the vertical asymptote $\beta = 2/Ra_r$. Thus, increasing the heat loss from the coal reduces the set of γ and β values for which multiplicity may occur. The data reported in appendix A show that for a typical coal $\gamma \approx 23.3$ and $\beta \approx 7$. This point falls within the multiplicity region for $Ra_r > 0.365$. Figure 1 is very useful for predicting whether multiplicity may occur for a specific coal, as it does not require knowledge of the reactivity, $k(T_a)$, of the specific coal.

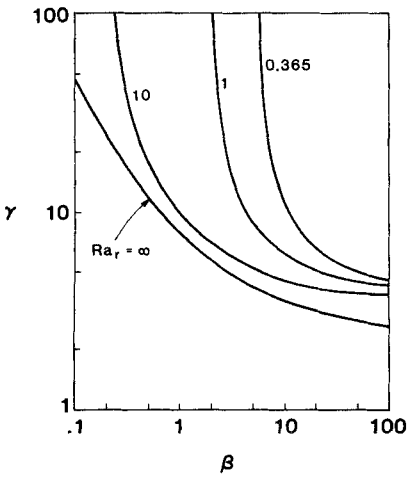

Figure 1. Uniqueness boundary for lumped thermal model for several Ra_r values.
A unique solution exists for (γ, β) values below or to the left of the boundary

Three solutions exist for a certain range of values of the Damkohler number Da_r (coal reactivities) when the γ and β values are above the uniqueness boundary for the proper Ra_r value. The boundaries of the multiplicity region in the (Da_r, Ra_r) plane for a specific set of γ and β values is the bifurcation set of Eq. 18. It is found by a simultaneous solution of Eq. 18 and

$$\frac{dG}{d\theta} = 0 \qquad (21)$$

A convenient way of constructing the bifurcation set is to compute it with the dimensionless temperature θ being a parameter along the curve. Figure 2 describes the bifurcation set for $\gamma = 23.3$ and $\beta = 7$. For sufficiently large values of Ra_r, the ignition occurs at $\theta = 1.0943$, $Y(1) = 0.9865$, and $Da_r/Ra_r = 1.43 \times 10^{-4}$ (point I), while the extinction is at $\theta = 7.18$, $Y(1) = 0.1170$, and $Da_r/Ra_r = 5.01 \times 10^{-10}$ (point E). Numerical calculations have shown that the temperature and the concentration vary in a nonmonotonic fashion along the bifurcation set. On the ignition branch IC, the temperature varies nonmonotonically from 1.0943 (point I) to 1.0771 (point C) with a minimum value of 1.0493. Along the extinction branch CE, θ varies monotonically from 1.0771 to 7.18.

The most important prediction of this lumped thermal model is that for sufficiently large values of Ra_r, the ignition as well as the extinction occur at a constant value of Da_r/Ra_r which depends only on the parameters γ and β.

In practice one may wish to change the coal particle size in order to avoid spontaneous ignition. Thus, it is essential to know the dependence of the bed temperature on the particle size. This dependence is usually presented as a bifurcation diagram of dimensionless temperature θ vs. a dimensionless particle size. Since both Da_r and Ra_r vary with the particle size, we reparameterize Eq. 16 by defining

$$D = Da_r\sqrt{Ra_r} = k(T_a)M\rho_a L\left(\frac{\epsilon^3 g c_p^3}{150\mu h^3}\right)^{0.5} \qquad (22)$$

Substitution of Eq. 22 into Eq. 16 gives a steady state equation with the parameters Ra_r, D, γ, and β. After this reparameteriza-

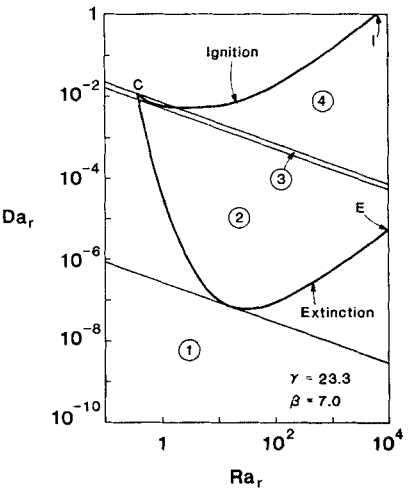

Figure 2. Bifurcation set of lumped thermal model.
Straight lines describe a path along which D is constant

tion, Ra_r is the only parameter that depends on the particle size. Thus, the bifurcation diagram of θ vs. Ra_r for a fixed set of (D, γ, β) may be constructed from Figure 2 by finding the values of θ and Ra_r as one moves along the straight line (on this log-log plot)

$$\log Da_r = -0.5 \log Ra_r + \log D \tag{23}$$

Several such paths are shown in Figure 2. It is very useful to be able to predict *a priori* the qualitative features of the bifurcation diagram for any set of parameters (γ, β, D). To accomplish this we use the scheme of Balakotaiah and Luss (1981) and construct two hypersurfaces that divide the global parameter space into regions with qualitatively different types of θ vs. Ra_r bifurcation diagrams.

The first surface is the hysteresis variety at which an ignition and extinction point coalesce. When the parameters cross this surface, a hysteresis loop in the θ vs. Ra_r diagram either appears or disappears. This surface consists of all the parameters for which

$$F = \frac{\partial F}{\partial \theta} = \frac{\partial^2 F}{\partial \theta^2} = 0 \tag{24}$$

Elimination of θ and Ra_r from Eqs. 24 gives the hysteresis variety in the (γ, β, D) space.

The second hypersurface is the isola variety, crossing which causes either the appearance (disappearance) of an isolated branch of solutions or an intersection of two branches of solutions and local separation into two isolated branches. That surface consists of all the parameters at which

$$F = \frac{\partial F}{\partial \theta} = \frac{\partial F}{\partial Ra_r} = 0 \tag{25}$$

Figure 3 shows a cross section of the hysteresis and isola varieties in the (γ, D) plane for $\beta = 7$. The hysteresis variety is in this case a single-valued line, while the isola variety forms a cusp. The two varieties intersect (Figure 3 inset) and divide the plane into five different regions. The qualitative features of the θ vs. Ra_r diagrams in each region are shown in the small diagrams at the top of Figure 3.

The θ vs. Ra_r bifurcation diagram is always single-valued and no ignition can occur for sufficiently low activation energies. An isolated ignited branch exists at large γ values for sufficiently low coal reactivity D. In this region a continuous extinguished branch exists and a spontaneous ignition requires a large perturbation of the bed temperature. In regions 3, 4, and 5 an ignition point exists at which a slight change in the particle size leads to a large jump in the bed temperature. Figure 3 suggests that for a typical coal ($\gamma \approx 23.3$) only the first four types of bifurcation diagrams are expected to exist, and that the bifurcation diagram of type 5 exists only in very narrow range of parameters.

The various paths in the (Da_r, Ra_r) plane, shown in Figure 2, correspond to parameters on one of the two varieties. The lower line, which is tangent to the extinction branch ($D = 2.914 \times 10^{-7}$), is on the isola variety and separates between parameters with bifurcation diagrams of type 1 and type 2. The second line, which is tangent to the ignition branch ($D = 5.278 \times 10^{-3}$), is on the branch of the isola variety and separates between bifurcation diagrams of type 2 and 3. The upper one for which $D = 6.946 \times$

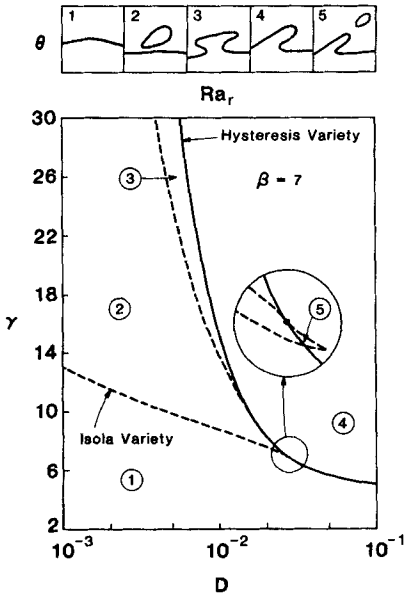

Figure 3. Classification of temperature θ vs. particle size Ra_r bifurcation diagrams for lumped thermal model.

10^{-3} (line through the cusp point of the bifurcation set), is on the hysteresis variety and separates between parameters with bifurcation diagrams of type 3 and 4.

The above analysis indicates that for a typical coal ($\gamma = 23.3$, $\beta = 7$) no ignition point is found if

$$D < 5.278 \times 10^{-3} \tag{26}$$

When the condition of Eq. 26 is violated there exists a critical particle size Ra_r below which ignition occurs. This value can be found from the intersection of the bifurcation set shown in Figure 2 with the straight line defined by Eq. 23. An analytical expression for the ignition point may be obtained using a simplification that is frequently used in the thermal explosion theory (Frank-Kamenetskii, 1939). The simplification assumes that on the extinguished (low-temperature) branch the reactant consumption is very low and $Y \approx 1$. Moreover, it is assumed that the dimensionless temperature rise is very small ($\theta - 1 \ll 1$), so that the Arrhenius temperature dependence can be replaced by the positive exponential approximation

$$\exp\left[\gamma\left(1 - \frac{1}{\theta}\right)\right] \approx e^{w} \tag{27}$$

where

$$w = \gamma(\theta - 1) \tag{28}$$

Using these assumptions, the steady state equation for the lumped thermal model simplifies to

$$\Delta = (2w + Ra_r^* w^2) \exp(-w) \equiv f_1(w) \tag{29}$$

where

$$\Delta = \gamma\beta Da_r \quad Ra_r^* = \frac{Ra_r}{\gamma} \tag{30}$$

At the ignition point, $f_1(w)$ has an extremum. This occurs at

$$w_i = 1 - \frac{1}{Ra_r^*} + \sqrt{1 + \frac{1}{(Ra_r^*)^2}} \tag{31a}$$

$$\Delta_i = 2[Ra_r^* + \sqrt{1 + (Ra_r^*)^2}] \cdot \exp\left[-1 + \frac{1}{Ra_r^*} - \sqrt{1 + \frac{1}{(Ra_r^*)^2}}\right] \tag{31b}$$

For sufficiently small values of the Rayleigh number Ra_r^*, the ignition point approaches the *conduction asymptote*

$$w_i = 1 \quad \Delta_i = 2e^{-1} = 0.736 \tag{32}$$

on which conduction is the main mechanism of heat removal, while for sufficiently large values of Ra_r^* it approaches the *convection asymptote*

$$w_i = 2 \quad \Delta/Ra_r^* = 4e^{-2} = 0.541 \tag{33}$$

on which natural convection is the main mechanism of heat loss. The ignition points, computed by Eq. 31b, are plotted in Figure 4, clearly showing the two asymptotes. The transition from the conduction asymptote to the convection asymptote occurs at Ra_r^* of order unity.

Bifurcation diagrams predicted by the lumped thermal model for a typical coal ($\gamma = 23.3, \beta = 7$) are shown in Figures 5 and 6. For sufficiently low reactivity, Eq. 26 is satisfied and an extinguished branch exists for all particle sizes, Figure 5. For higher reactivities, ignition occurs at some critical particle size, Figure 6.

While this model is expected to predict rather well the qualitative features, it does not adequately describe the quantitative features, especially the ignited states in which large temperature gradients exist.

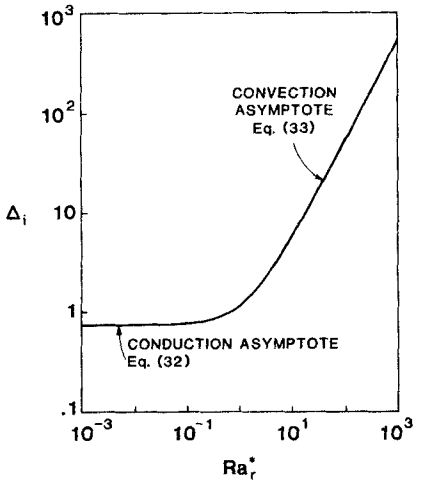

Figure 4. Locus of ignition points for lumped thermal model.

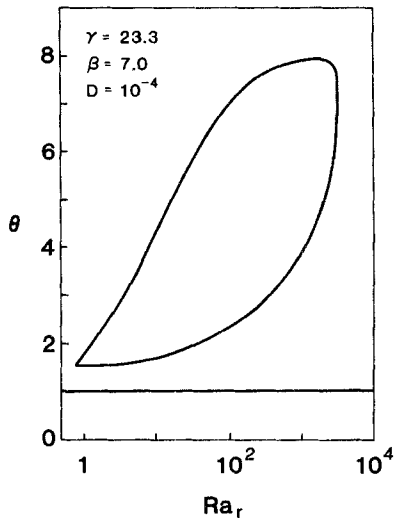

Figure 5. Typical bifurcation diagram of lumped thermal model for low reactivity.

Plug-flow model

The second limiting model, called the plug-flow model, is obtained when the characteristic time for natural convection t_c is much smaller than that for heat conduction t_λ and heat loss t_r. In this case the energy balance, Eq. 11, may be simplified to

$$\frac{d\theta}{dX} = \frac{\beta\phi_h^2}{S} \exp\left[\gamma\left(1 - \frac{1}{\theta}\right)\right] Y \tag{34}$$

subject to the boundary condition

$$\theta = 1 \quad X = 0 \tag{35}$$

Combining Eqs. 10 and 34 and integrating gives the invariant

$$Y = (1 + \beta - \theta)/\beta \tag{36}$$

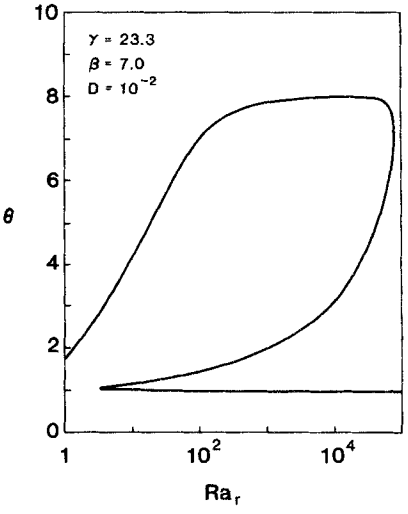

Figure 6. Typical bifurcation diagram of lumped thermal model for high reactivity.

Substituting Eq. 36 into Eq. 34 and integrating gives

$$I_o(\theta_1, \gamma, \beta) - \frac{\phi_h^2}{S} = 0 \tag{37}$$

where we define

$$I_j(\theta_1, \gamma, \beta) = \int_1^{\theta_1} \frac{\theta^j \exp(-\gamma + \gamma/\theta)}{(1 + \beta - \theta)}\, d\theta \tag{38}$$

and θ_1 is the dimensionless temperature at the top of the coal layer [$\theta_1 = \theta(1)$]. Dividing Eq. 34 by Eq. 12 and integrating, we get

$$S = Ra\left[\frac{I_o(\theta_1, \gamma, \beta) - I_{-1}(\theta_1, \gamma, \beta)}{I_1(\theta_1, \gamma, \beta)}\right] \tag{39}$$

Substitution of Eq. 39 into Eq. 37 gives the steady state equation

$$F(\theta_1, Da_c, \gamma, \beta) \equiv I_o^2 - I_o I_{-1} - Da_c I_1 \equiv 0 \tag{40}$$

where we define

$$Da_c = \frac{\phi_h^2}{Ra} = \frac{t_c}{t_g} = \frac{150k(T_a)LM\mu(1-\epsilon)^3}{\rho_a^2 g D_p^3 \epsilon^3} \tag{41}$$

The arguments of I_j have been dropped for convenience. Note that the parameters in this limiting model are independent of the characteristic times t_λ and t_r.

Analysis of Eq. 40 indicates that $\theta \to 1$ as $Da_c \to 0$ and that $\theta \to 1 + \beta$ as $Da_c \to \infty$. Thus, this model predicts complete conversion for very small particles ($Da_c \to \infty$), for which the natural convection flow is very slow. However, it should be noted that the assumptions on which this model is based are not satisfied for very small particle sizes.

It follows from Eq. 40 that

$$\frac{\partial F}{\partial Da_c} = -I_1 \neq 0 \tag{42}$$

so that Da_c is a single-valued function of θ_1. (This may also be seen by rewriting Eq. 40.) Thus, a bifurcation diagram of θ_1 vs. Da_c, or equivalently of θ_1 vs. Ra for a fixed D^* cannot have an isolated branch, where

$$D^* = \phi_h^2\sqrt{Ra} = k(T_a)M\rho_a\left(\frac{\epsilon^3 g c_p^3 L^5}{150\mu k_e^3}\right)^{0.5} \tag{43}$$

Figure 7 shows the numerically computed hysteresis variety in the (γ, β) plane. The bifurcation diagram of θ vs. Ra has an inverse S shape, with three solutions for a bounded range of Ra values for all (γ, β) to the right of the variety. θ is a single-valued function of Ra for all (γ, β) to the left of the hysteresis variety.

Figure 7 shows that for $\gamma = 23.3$ and $\beta = 7$, multiplicity does not exist for any Ra. We conclude that for a typical coal this model predicts that a unique solution exists for all Ra.

While the plug-flow model predicts that steady state multiplicity does not occur for $\gamma = 23.3$ and $\beta = 7$, it reveals a rapid

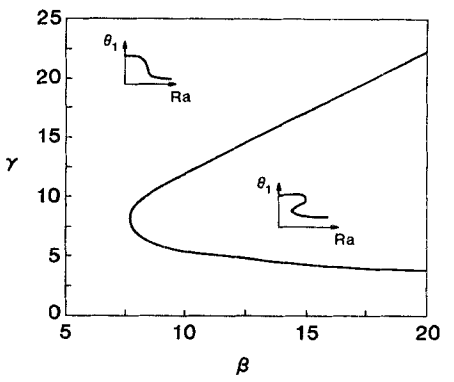

Figure 7. Uniqueness boundary for plug-flow model.

change in the value of θ_1 at some Da_c value, as illustrated in Figure 8. The practical impact of this parametric sensitivity (rapid shift to high θ_1 value) is similar to that of the ignition. Thus, it is of interest to predict the Da_c value at which this occurs. The approximate location of this point may be predicted analytically by using the positive exponential approximation and neglecting reactant consumption. Under these assumptions, Eq. 40 simplifies to

$$\gamma^2\beta Da_c = \int_0^{w_1} we^{-w}\, dw \tag{44}$$

where

$$w_1 = \gamma(\theta_1 - 1) \tag{45}$$

When the mathematical model of an adiabatic reactor does not account for reactant consumption, parametric sensitivity implies that the temperature becomes unbounded. It follows from Eq. 44 that parametric sensitivity appears ($w_1 \to \infty$) when

$$\gamma^2\beta Da_c = \int_0^{\infty} we^{-w}\, dw = 1 \tag{46}$$

Using the same assumptions and Eq. 46, one can use Eq. 39 to show that at the point of parametric sensitivity the velocity

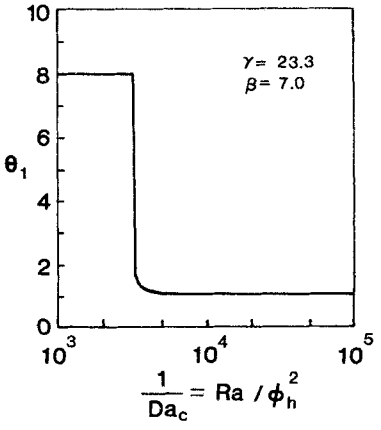

Figure 8. Bifurcation diagram for plug-flow model.

through the bed is

$$u_o^* = \frac{\kappa g \rho_a}{\mu \gamma} = \frac{L}{\gamma t_c} \tag{47}$$

The above simplifying procedure may be used to show that the onset of parametric sensitivity in a plug-flow, adiabatic reactor occurs when

$$\gamma \beta Da^* = 1 \tag{48}$$

where $Da^* = t_c^*/t_g^*$.

We note that if

$$Da^* = \beta Da_c \tag{49}$$

the criteria of Eqs. 46 and 48 are identical. Thus, the onset of parametric sensitivity in a coal pile is the same as that in a plug-flow, adiabatic reactor in which t_g^* is the same as t_g defined by Eq. 9 and the forced velocity is equal to natural convection velocity u_o^* defined by Eq. 47. For $\gamma = 23.3$, $\beta = 7$, Eq. 46 predicts a rapid increase in the θ value at $Da_c = 2.63 \times 10^{-4}$, while the exact value is 3.08×10^{-4}.

Dirichlet model

The third limiting model, called the Dirichlet model, describes cases in which the characteristic time for heat loss t_r is much smaller than that for heat conduction t_λ or natural convection t_c, so that the temperature at the ends of the bed is nearly equal to the ambient value. In this case, the boundary conditions, Eqs. 13a and 14a, may be replaced by

$$\theta = 1; \quad X = 0 \tag{50a}$$

$$\theta = 1; \quad X = 1 \tag{50b}$$

This limiting model contains four parameters (γ, β, ϕ_h^2, Ra), as compared to the five parameters in the general model.

The numerical computation of the limit (ignition and extinction) points and the hysteresis and isola varieties of this model is much more cumbersome and time-consuming than that of previous two limiting cases. The details of the calculations are described in appendix B.

Numerical calculations have shown that the qualitative features of this model for a typical coal were rather similar to those of the lumped thermal model; that is, similar bifurcation diagrams exist for both models. Figure 9 shows the numerically computed bifurcation set in the (ϕ_h^2, Ra) space. For sufficiently large values of the Rayleigh number Ra, the ignition occurs at $\phi_h^2/Ra = 3.0 \times 10^{-4}$, which is also the condition at which parametric sensitivity appears in the plug-flow model.

The region of D^* values for which an extinguished state exists for all particle sizes may be determined by computing the segment of the isola variety along which two ignition points appear (isola to mushroom transition). This can be found from the intersection of the ignition locus with the line

$$\log \phi_h^2 = -0.5 \log Ra + \log D^* \tag{51}$$

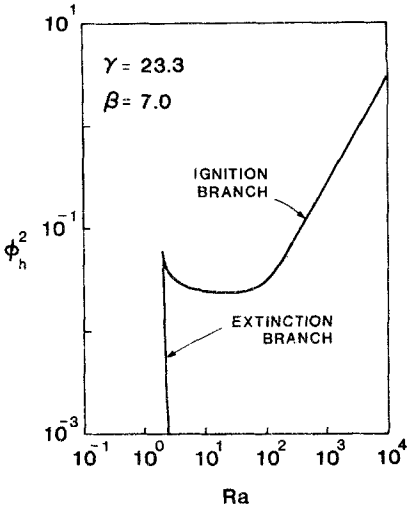

Figure 9. Bifurcation set for Dirichlet model.

No ignition point is found for parameter values of a typical coal if

$$D^* < 0.057 \tag{52}$$

When the condition of Eq. 52 is violated, there exists a critical particle size Ra below which only an ignited state exists. An accurate estimate of this ignition point may be obtained using the simplification described in the analysis of the lumped thermal model. Specifically, we neglect reactant consumption and use the positive exponential approximation. In addition, we simplify the momentum balance equation by assuming a constant frictional pressure gradient, i.e.,

$$\frac{d\Pi}{dX} = -\frac{S}{Ra} + \frac{w}{\gamma} \tag{53}$$

Integration of Eq. 53 subject to boundary condition Eqs. 13c and 14b gives the following relation for the velocity

$$S = Ra^* \langle w \rangle \tag{54}$$

where $Ra^* = Ra/\gamma$, and $\langle w \rangle$ denotes the average value of w in the bed, i.e.,

$$\langle w \rangle = \int_0^1 w \, dX \tag{55}$$

Using Eqs. 27, 28, and 53, the energy balance may be rewritten as

$$\frac{d^2w}{dX^2} - Ra^* \langle w \rangle \frac{dw}{dX} + \delta \exp(w) = 0 \tag{56}$$

where

$$\delta = \gamma \beta \phi_h^2 \tag{57}$$

The corresponding boundary conditions are

$$w = 0; \quad X = 0 \tag{58a}$$

$$w = 0; \quad X = 1 \tag{58b}$$

The ignition point of the two-point boundary value problem defined by Eqs. 56 and 58 was determined by the method developed by Witmer et al. (1986). Figure 10 shows the numerically computed ignition locus in the (δ, Ra^*) plane. For sufficiently small values of the Rayleigh number Ra^* the ignition locus approaches the conduction asymptote $\delta = 3.514$, while for $Ra^* \gg 1$ it approaches the convection asymptote $\delta = Ra^*$. The figure indicates that the two asymptotes provide an adequate approximation of the exact value. The maximal deviation of about 18% is at the corner point, at which the two asymptotes intersect.

Analysis of the General Model

When the conduction, convection, and cooling (radiation) time scales are of the same order of magnitude, Eqs. 10–14 contain five parameters (γ, β, ϕ_h^2, Ra, Bi) and must be solved numerically using the method outlined in the previous section. The qualitative features of the general model are found to be similar to those of the lumped thermal and Dirichlet models and approach these limiting cases when one time scale is much smaller than the other two.

Figure 11 shows the boundary at which the isola to mushroom transition occurs in the (D^*, Bi) plane for a typical coal (γ = 23.3, β = 7.0). This numerically computed boundary can be approximated rather closely by the two asymptotes describing the lumped thermal and Dirichlet models.

The numerically computed ignition locus of the general model for $\gamma = 23.3$, $\beta = 7.0$, and $Bi = 156.0$ is shown in Figure 12. As in the limiting models discussed above, the ignition occurs at a constant value of ϕ_h^2/Ra for sufficiently large values of the Rayleigh number. When this figure is replotted in the (δ, Ra^*) plane the ignition locus for $Bi = 156$ is practically indistinguishable from that of the Dirichlet model shown in Figure 10.

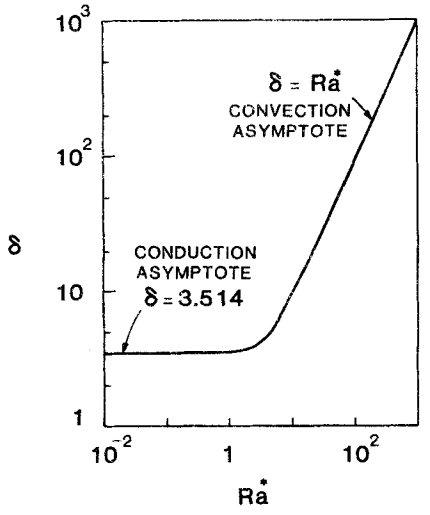

Figure 10. Approximate locus of ignition points for Dirichlet model.

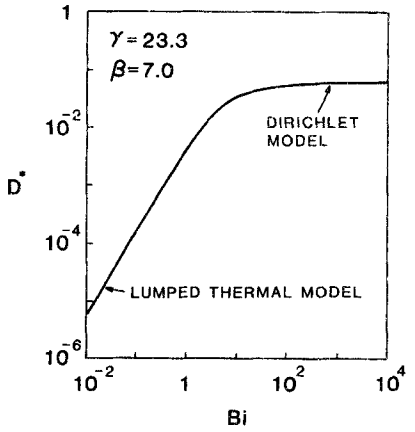

Figure 11. Boundary at which isola to mushroom transition occurs for general model.
Ignition does not occur for parameters below or to the right of the boundary

The approximate location of the ignition locus of the general model can be computed by Eq. 56, subject to the boundary conditions

$$\frac{dw}{dX} = (Bi + Ra^*\langle w \rangle)w; \quad X = 0 \tag{59a}$$

$$\frac{dw}{dX} = -Biw; \quad X = 1 \tag{59b}$$

It is convenient to plot the ignition locus of Eqs. 56 and 59 in the (δ, Ra^*) plane for a fixed value of Bi (which is independent of the particle size). For sufficiently small values of Ra^* the ignition locus is independent of the Rayleigh number and occurs at a constant δ value. This asymptotic value can be obtained from the solution of the Frank-Kamenetskii problem obtained by setting $Ra^* = 0$ in Eqs. 56 and 59. A parametric representation of the

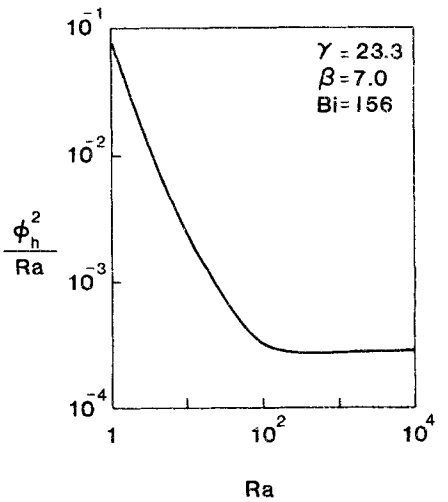

Figure 12. Locus of ignition points for general model.

ignition point is given by

$$Bi = \frac{2c(\tanh c + c\,\mathrm{sech}^2 c)}{(1 - c\tanh c)} \tag{60a}$$

$$\delta = 8c^2\,\mathrm{sech}^2 c\,\exp\left(-\frac{4c\tanh c}{Bi}\right) \qquad (0 < c < 1.1996786) \tag{60b}$$

For $Bi \gg 1$, δ approaches the Frank-Kamenetskii limit of 3.514, while for $Bi \ll 1$ the ratio (δ/Bi) approaches the Semenov (lumped thermal) limit of 0.736. We refer to the boundary defined by Eq. 60 as the conduction asymptote. Physically, this boundary corresponds to cases in which the natural convection does not affect the ignition. Many experimental studies of thermal explosion verified the above prediction of ignition by the Frank-Kamenetskii analysis.

When the Rayleigh number is sufficiently large ($Ra^* \gg 1$), the conduction term is much smaller than the convection term in Eq. 56. Dropping this term and integrating the resulting equation subject to the boundary condition $w(0) = 0$, gives Eq. 46. Thus, any ignition point has to lie below the line $\gamma^2\beta Da_c = 1$, or equivalently, $\delta = Ra^*$ for $Ra^* \gg 1$.

The numerically computed ignition points of Eqs. 56 and 59 are shown in Figure 13 for $Bi = 0.1, 1, 10, 100$. The calculations show that for sufficiently large values of the Rayleigh number Ra^*, the ignition locus is nearly independent of the Biot number and is given by $\delta \approx Ra^*$, or equivalently, $Ra = \gamma^2\beta\phi_h^2(Da_c\gamma^2\beta = 1)$. In terms of characteristic times this transition to ignition can be written as

$$\frac{t_g}{t_c} = \gamma^2\beta = \frac{1}{Da_c} \tag{61}$$

This relation for the convection asymptote under vigorous natural convection ($Ra^* \gg 1$) is identical to the one obtained for the onset of parametric sensitivity in an adiabatic, plug-flow reactor in which the forced velocity is given by Eq. 47. As expected, the ignition at high Rayleigh members is unaffected by the characteristic times for conduction and heat removal from the surface. In terms of the physical parameters, the criterion of Eq. 61 predicts that ignition will occur if

$$\frac{\gamma^2 Q(T_a)\mu L}{\rho_a^2 c_p T_a g\kappa} > 1 \tag{62}$$

where $Q(T_a)$ is the observed rate of heat generation at ambient temperature per unit volume of bed $[=(-\Delta H)r(T_a)]$. This is a very useful criterion which predicts the dependence of the ignition on the temperature sensitivity of the reaction rate γ, the observed heat production rate, and the physical properties of the gas, bed length, and permeability. In practice, Ra^* is usually larger than four so that criterion Eq. 62 defines the ignition.

When the coal particles are nonporous the reaction rate is defined by Eq. 4b, and criterion Eq. 62 can be used to show that ignition occurs for particle sizes satisfying the condition

$$D_p < D_{pi} \triangleq \left(\frac{1-\epsilon}{\epsilon}\right)\left[\frac{150\gamma^2\beta\mu k(T_a)LM}{g\rho_a^2}\right]^{1/3} \tag{63}$$

Equation 63 yields two important conclusions:

1. The particle size at ignition is proportional to $(1 - \epsilon)/\epsilon$. Thus, the lower the void fraction of the bed, the higher is the particle size at which ignition occurs.

2. The particle size at ignition is proportional to the cubic root of the bed size and coal reactivity under ambient conditions. Thus, for a coal with a specific preexponential factor, increasing the ambient temperature shifts the ignition to larger particle size. Figure 14 illustrates this impact of ambient temperature on the critical particle size for coal piles made up of different sized nonporous particles.

Conclusions and Remarks

The three limiting models analyzed in this work enabled us to gain important insights into the structure of the solutions of the general model. In practice, the Rayleigh number is usually much larger than unity, and the asymptotic ignition locus predicted by both the Dirichlet and the lumped thermal models

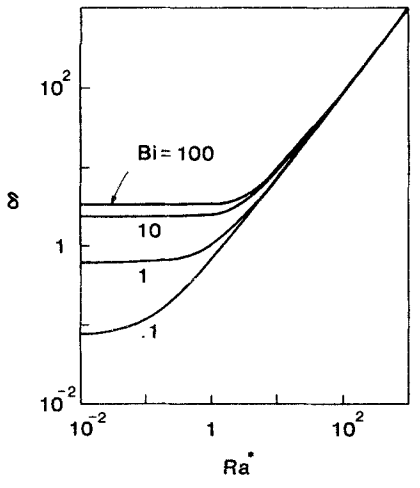

Figure 13. Ignition locus for general model with no reactant consumption and positive exponential approximation.

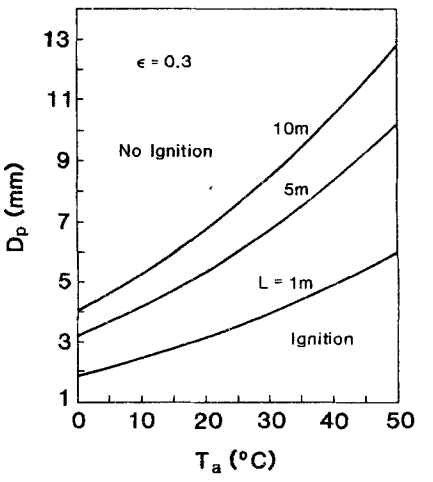

Figure 14. Ignition boundary in particle size D_p–ambient temperature T_a plane for coal beds of different size.

bounds the value predicted by the general model. Since $Bi \gg 1$ under practical conditions, the ignition locus of the general model is very close to that predicted by the Dirichlet model. The simple criterion defined by Eq. 62 is useful for predicting the impact of a change in the properties of the coal or the pile on ignition.

The models presented in this work ignore the oxygen diffusion term, which becomes important at small Rayleigh numbers. The addition of this term to the species balance is not expected to change the predicted ignition locus (for small Rayleigh numbers) since the reactant consumption is very low at ignition. However, at least part of the mushroom to isola transition (isola variety) is predicted to exist at small Rayleigh numbers, at which the contribution of oxygen diffusion is no more negligible in comparison to that by natural convection and the conversion is not very small. Thus, the prediction of this boundary, in contrast to that of the ignition, may be rather sensitive to the oxygen diffusion term.

One may obviously devise more complex and realistic models of coal stockpiles. The solution of these models will necessarily require numerical computations. The simple models presented here should provide helpful guidance and insight into the behavior of these complex models. It is important to remember that any model of a coal stockpile involves some uncertainties due to the lack of uniformity in the properties of the pile and the coal. We expect the refined model to predict essentially the same qualitative features as the simple models presented here. Thus, the inherent uncertainties raise the question whether the use of more complex model is warranted in this case, and whether it will actually improve the quantitative predictions.

The present one-dimensional model disregards processes such as water absorption and intraparticle diffusion and reaction and potential changes of coal reactivity with time. Further analysis and experimental information is needed in order to check the qualitative and quantitative impact of these simplifications on the predicted ignition features. It is especially important to find out if any of these simplifications, or the use of the simplified one-dimensional geometry, may lead to erroneous predictions of the qualitative impact of a change in the operating condition or properties of the coal pile on ignition. This point clearly requires further investigation before such models and analyses may be used confidently to predict the behavior of stockpiled coal.

In the analysis we refer only to coal piles. However, the same model and criteria are applicable to other piles of self-heating combustible materials, such as grain, oil seeds, biological or waste dumps, and so forth.

Acknowledgment

This work was made possible by assistance to Kevin Brooks from both the Council for Scientific and Industrial Research and the University of Witwatersrand, Johannesburg, South Africa. We also wish to acknowledge the support of the ACS-PRF and the Energy Laboratory of the University of Houston.

Notation

a = surface area per unit volume of bed
c_p = gas specific heat per unit mass
D = dimensionless parameter, Eq. 22
D^* = dimensionless parameter, Eq. 43
Da_r = Damköhler number, Eq. 17
Da_c = Damköhler number, Eq. 41
Da^* = Damköhler number for plug flow reactor
D_p = particle size
E = activation energy
f_p = frictional pressure gradient
g = acceleration due to gravity
G = function, Eq. 18
h = heat transfer coefficient
$(-\Delta H)$ = enthalpy of reaction, J/kmol
I_j = integral, Eq. 38
$k(T)$ = reaction rate constant at temperature T
k_e = bed thermal conductivity
k_o = preexponential factor
L = bed length
M = molecular weight
P^* = excess bed pressure over the ambient pressure
p = vector of parameters
Q = observed rate of heat generation per unit volume
R = universal gas constant
Ra = Rayleigh number, Eq. 9
Ra_r = Rayleigh number, Eq. 17
Ra^* = modified Rayleigh number, $Ra^* = Ra/\gamma$
r = rate of reaction
S = dimensionless velocity
t_c = characteristic time for natural convection
t_λ = characteristic time for heat conduction
t_g = characteristic time for heat generation
t_r = characteristic time for heat removal
T = bed temperature
u = velocity
u^* = velocity of onset of parametric sensitivity, Eq. 47
U_r = reference velocity, Eq. 9
w = dimensionless temperature, Eq. 28
X = dimensionless coordinate
x = distance from bed inlet
Y = oxygen mole fraction divided by ambient value
y = oxygen mole fraction

Greek letters

δ = Frank-Kamenetskii parameter, Eq. 57
Δ = quantity, Eq. 30
β = dimensionless adiabatic temperature rise
γ = dimensionless activation energy
ϵ = bed voidage
μ = gas viscosity
Π = dimensionless pressure
κ = permeability of bed
ρ = density
θ = dimensionless temperature

Subscripts

0 = bed entrance
1 = bed exit
a = ambient
i = ignition

Appendix A

Parameter values for typical coal

$$\text{Rate} = k(T_a)(1-\epsilon)\left(\frac{y}{D_p}\right)\exp\left(\frac{E}{RT_a}-\frac{E}{RT}\right)$$

$$k(T_a) = 6k_o\rho_a \exp\left(-E/RT_a\right)/M$$

$$k_o = 10 \text{ m/s}$$

$$T_a = 300 \text{ K}$$

$$E/R = 7{,}000 \text{ K}$$

$$\rho_a = 1.18 \text{ kg/m}^3$$

$$M = 29.0$$

$$g = 9.8\ \text{m/s}^2$$

$$\epsilon = 0.3$$

$$\mu = 1.8 \times 10^{-5}\ \text{kg/m} \cdot \text{s}$$

$$(-\Delta H) = 3 \times 10^8\ \text{(J/kmol)}$$

$$Mc_p = 3 \times 10^4\ \text{J/kmol} \cdot \text{K}$$

$$y_a = 0.21$$

$$k_e = 0.2\ \text{W/m} \cdot \text{K}$$

$$L = 1.0\ \text{m to } 10.0\ \text{m}$$

$$h = 5.0 \text{ to } 10.0\ \text{W/m}^2 \cdot \text{K}$$

$$D_p = 1.0 \text{ to } 20.0\ \text{mm}$$

$$Q(T_a) = 0.1 \text{ to } 1.0\ \text{W/m}^3$$

Dimensionless parameters

$$\gamma = 23.3$$

$$\beta = 7.0$$

$$Bi = 25 \text{ to } 500$$

$$\phi_h^2 = 0.01 \text{ to } 1.0$$

$$Ra = 10 \text{ to } 10^4$$

Appendix B

Calculation of singular points of Eqs. 10–14

The boundary value problem defined by Eqs. 10–14 may be recast as an initial value problem by assuming the values of $\theta_1' \equiv d\theta(1)/dX$, $Y_1 \equiv Y(1)$, and S, and integrating the three differential equations backward from $X = 1$ to $X = 0$. Backward integration must be used since the forward integration scheme is unstable (Coste et al., 1963). The three unknowns are found by solving the following three implicit algebraic equations (boundary conditions at $X = 0$):

$$F_1(\theta_1', Y_1, S, Ra, p) \equiv \theta(X = 0) - 1 - \frac{1}{(S + Bi)} \frac{d\theta}{dX}(X = 0) = 0 \quad \text{(B1)}$$

$$F_2(\theta_1', Y_1, S, Ra, p) \equiv Y(X = 0) - 1 = 0 \quad \text{(B2)}$$

$$F_3(\theta_1', Y_1, S, Ra, p) \equiv \Pi(X = 0) = 0 \quad \text{(B3)}$$

where θ_1', Y_1, and S are the state variables, Ra is the bifurcation variable, and

$$p = (\gamma, \beta, D^*) \quad \text{(B4)}$$

is the parameters vector with D^* defined by Eq. 42. For the Dirichlet model, the last term in Eq. B1 must be dropped. Equations B1–B3 were solved numerically using a modified Newton's iteration method with the Jacobian matrix generated numerically. The package DGEAR (Hindmarsh, 1974) was used to integrate the stiff initial value problems.

At a limit (ignition or extinction) point the following criterion must be satisfied at $X = 0$:

$$F_4(\theta_1', Y, S, Ra, p) \equiv \begin{vmatrix} \frac{\partial F_1}{\partial \theta_1'} & \frac{\partial F_1}{\partial Y_1} & \frac{\partial F_1}{\partial S} \\ \frac{\partial F_2}{\partial \theta_1'} & \frac{\partial F_2}{\partial Y_1} & \frac{\partial F_2}{\partial S} \\ \frac{\partial F_3}{\partial \theta_1'} & \frac{\partial F_3}{\partial Y_1} & \frac{\partial F_3}{\partial S} \end{vmatrix} = 0 \quad \text{(B5)}$$

To find these partial derivatives we need to compute the following 12 sensitivity functions associated with Eqs. 10–14:

$$p_1 = \frac{\partial Y}{\partial \theta_1'} \quad p_2 = \frac{\partial Y}{\partial Y_1} \quad p_3 = \frac{\partial Y}{\partial S}$$

$$q_1 = \frac{\partial \theta}{\partial \theta_1'} \quad q_2 = \frac{\partial \theta}{\partial Y_1} \quad q_3 = \frac{\partial \theta}{\partial S}$$

$$r_1 = \frac{\partial v}{\partial \theta_1'} \quad r_2 = \frac{\partial v}{\partial Y_1} \quad r_3 = \frac{\partial v}{\partial S}$$

$$s_1 = \frac{\partial \Pi}{\partial \theta_1'} \quad s_2 = \frac{\partial \Pi}{\partial Y_1} \quad s_3 = \frac{\partial \Pi}{\partial S} \quad \text{(B6)}$$

where

$$v = \frac{d\theta}{dX} \quad \text{(B7)}$$

The equations and initial conditions defining the sensitivity functions are found by differentiation of Eqs. 10–12 and 14. The 12 initial value problems for the sensitivity functions are integrated along with Eqs. 10–12 to find the values of the state variables and sensitivity functions at $X = 0$. Thus, in order to evaluate $F_i (i = 1 \text{ to } 4)$, 16 first-order equations need to be integrated. The limit-point coordinates were found by using a modified Newton's method with a numerically generated Jacobian matrix. An arc-length continuation scheme was used to determine the locus of such points.

The above procedure was reasonably efficient for computing the ignition points. However, it was not possible to compute the complete extinction locus. The reason is that the very steep temperature and oxygen concentration profiles for the ignited states make the equations stiff and difficult to integrate accurately.

The hysteresis and isola varieties were computed by utilizing the fact that in the (Da_c, Ra) plane, a minimum in the locus of limit points is an isola point and a cusp is a hysteresis point. Thus, the varieties may be generated by repeated computation of the locus of limit points.

Literature Cited

Balakotaiah, V., and D. Luss, "Analysis of the Multiplicity Patterns of a CSTR," *Chem. Eng. Commun.*, **11**, 111 (1981).

Bowes, P. C., *Self-Heating: Evaluating and Controlling the Hazards,"* Elsevier, New York (1984).
Brooks, K., and D. Glasser, "A Simplified Model of Spontaneous Combustion in Coal Stockpiles," *Fuel,* **65,** 1035 (1986).
Coste, P., D. Rudd, and N. R. Amundson, "Taylor Diffusion in Tubular Reactors," *Can. J. Chem. Eng.,* **39,** 149 (1963).
Frank-Kamenetskii, D. A., "Calculation of Thermal Explosion Limits," *Acta. Phys.-Chim, URSS,* **10,** 365 (1939).
Hindmarsh, A. C., "GEAR: Ordinary Differential Equation System Solver," Lawrence Livermore Laboratory, Rept. UCID-30001 (1974).
Hlavacek, V., and J. Votruba, in *Chemical Reactor Theory—A Review,* L. Lapidus, N. R. Amundson, eds., Prentice-Hall, Englewood Cliffs, NJ, ch. 6, 314–404 (1977).
Itay, M., "The Low-Temperature Oxidation of Coal: Its Kinetics and Implications for Spontaneous Combustion," Ph.D. Thesis, Univ. Witwatersrand, Wits, S. Africa (1984).
Kordylewski, W., and Z. Krajewski, "Convection Effects on Thermal Ignition in Porous Media," *Chem. Eng. Sci.,* **39,** 610 (1984).
Lee, J. P., V. Balakotaiah, and D. Luss, "Thermoflow Multiplicity in a Packed-Bed Reactor," *AIChE J.,* Part I in **33**(7), 1136 (July, 1987) and Part II in **34**(1), 37 (Jan. 1988).
Merzhanov, A. G., and E. A. Shtessel, "Free Convection and Thermal Explosion in Reactive Systems," *Acta Astronautica,* **18,** 191 (1973).
Nordon, P., "A Model for the Self-Heating Reaction of Coal and Char," *Fuel,* **58,** 456 (1979).
Schmal, D., J. H. Duyzer, and J. W. van Heuven, "A Model for the Spontaneous Heating of Coal," *Fuel,* **64,** 963 (1985).
Schmidt, L. D., and J. L. Elder, "Atmospheric Oxidation of Coal at Moderate Temperatures; Rates of Oxidation Reaction for Representative Coking Coals," *Ind. Eng. Chem.,* **32,** 249 (1940).
Sondreal, E. A., and R. C. Ellman, U. S. Bureau of Mines, Report of Investigations 7887 (1974).
Varma, A., and R. Aris, "Stirred Pots and Empty Tubes," *Chemical Reactor Theory,* L. Lapidus, N. R. Amundson, eds., McGraw-Hill, New York (1977).
Viljoen, H., and V. Hlavacek, "Chemically Driven Convection in a Porous Medium," *AIChE J.,* **33,** 1344 (1987).
Young, B. D., D. F. Williams, and A. W. Bryson, "Two-Dimensional Natural Convection and Conduction in a Packed Bed Containing a Hot Spot and Its Relevance to the Transport of Air in a Coal Dump," *Int. J. Heat Mass Trans.,* **29,** 331 (1986).
Witmer, G. S., V. Balakotaiah, and D. Luss, "Multiplicity Features of Distributed Systems. I: Langmuir Hinshelwood Reaction in a Porous Catalyst," *Chem. Eng. Sci.,* **41,** 179 (1986).

Manuscript received Sept. 8, 1987, and revision received Nov. 4, 1987.